

## REVIEW

View Article Online  
View Journal | View IssueCite this: *Mater. Chem. Front.*,  
2020, 4, 128

# Förster resonance energy transfer (FRET) paired carbon dot-based complex nanoprobe: versatile platforms for sensing and imaging applications

Shihai Miao,<sup>a</sup> Kang Liang <sup>bc</sup> and Biao Kong <sup>\*a</sup>

As one of the most promising carbon-based photoluminescent materials, carbon dots (CDots) have recently attracted great attention for many potential applications owing to their excellent optical, electrical, and chemical properties. Förster Resonance Energy Transfer (FRET) is a highly sensitive spectroscopic technique that has been widely utilized for all applications of fluorescence. In this review, we provide an updated roadmap of CDot-based FRET systems for nanoprobe. Several CDot-based FRET systems obtained by co-assembling different fluorescent molecules are surveyed. Furthermore, the synthesis strategies for CDot-based FRET systems and their applications in nanoprobe, bioimaging, and biomedicine are reviewed. We further provide an outlook toward the future development of CDot-based FRET systems. This article summarizes the latest progress in CDot-based FRET systems and looks forward to further developments in these exciting nanocomposites.

Received 25th August 2019,  
Accepted 3rd October 2019

DOI: 10.1039/c9qm00538b

rsc.li/frontiers-materials

## 1. Introduction

Förster resonance energy transfer (FRET) is the mechanism by which non-radiative energy is transferred between a luminescent donor and an energy acceptor within a close range of approximately 10 to 100 Å.<sup>1–3</sup> FRET can be easily measured in standard bulk fluorescence experiments. FRET can also be monitored using fluorescence microscopy techniques, including single-molecule fluorescence spectroscopy. FRET serves as a highly sensitive spectroscopic technique that has been widely utilized in all applications of fluorescence, including medical

<sup>a</sup> Department of Chemistry, Collaborative Innovation Center of Chemistry for Energy Materials (iChEM), Laboratory of Advanced Materials, Shanghai Key Laboratory of Molecular Catalysis and Innovative Materials, Fudan University, Shanghai 200433, P. R. China. E-mail: bkong@fudan.edu.cn; Web: <https://softnanolab.fudan.edu.cn>; Fax: +86-21-31249176; Tel: +86-21-31249176

<sup>b</sup> School of Chemical Engineering, Graduate School of Biomedical Engineering, The University of New South Wales, Sydney NSW 2052, Australia

<sup>c</sup> Australian Centre for NanoMedicine, The University of New South Wales, Sydney NSW 2052, Australia



Shihai Miao

Shihai Miao obtained a bachelor's degree (2013) in Materials Chemistry at China University of Geosciences (Beijing) and a master's degree (2016) in Materials Engineering at China University of Geosciences (Beijing). He is currently an assistant researcher under the supervision of Prof. Dr Biao Kong in the Soft Nano Group at Fudan University. His research is focused on the design, synthesis, and characterization of carbon nanodots for applications in biosensing and flexible display devices.



Kang Liang

Dr Kang Liang is a specially invited researcher and Scientia Fellow in the department of Chemical Engineering and Biomedical Engineering at The University of New South Wales. He received a Bachelor of Engineering degree with Honors (Biomedical) in 2009 from the University of Melbourne (Australia) and commenced his PhD in 2010 under the supervision of Professor Frank Caruso. His research interests are primarily focused on the application of advanced bio-nano interface materials in biomedicine.

diagnosis, biological analysis, and optical imaging.<sup>4–7</sup> FRET-based dual-emission nanoprobe for ratiometric fluorescence sensing are achieved by synthesizing nanoparticles from two or more fluorescent molecules with different emission bands. One fluorophore serves as the reference, while the other acts as a response molecule, allowing the FRET system to be used as a ratiometric fluorescence nanoprobe. To date, many excellent studies and reviews of FRET have been conducted. In 2013, Chen *et al.* reviewed fluorescent nanosensors based on FRET. This review introduced the design and applications of sensitive and selective FRET-based ratiometric nanoprobe in detail. This review also classified nanosensors based on the type of nanoparticle and demonstrated the design and application of FRET-based fluorescent nanosensors for the detection of metal ions, small molecules, DNA, and other analytes.<sup>17</sup> In 2014, Prevo *et al.* reviewed FRET and kinesin motor proteins. The physical basis of FRET and how to apply FRET to biological molecules was systematically introduced. Prevo *et al.* focused on the application of different FRET methods in motor protein drivers that had undergone several conformational changes under the action of enzymes. This FRET system moves unidirectionally along the microtubule filament, driving active intracellular transport.<sup>18</sup> In 2014, Algar *et al.* examined the applications of FRET systems based on semi-conductor quantum dots. They reviewed the characterization of non-traditional structures of quantum dot-based FRET systems and their applications in biosensors, energy conversion, and optoelectronic device manufacturing in recent years.<sup>19</sup> Although many applications of FRET have been reported, it is still an analytical tool that must continue to be developed. For example, the study of new energy-transfer donor and receptor pairs in the FRET system is important to improve FRET efficiency and analytical performance.

Carbon dots (CDots) are newly emerging carbon-based fluorescent nanomaterials that have received considerable

attention in recent years. Owing to their high optical stability, ease of synthesis and surface functionalization, good biocompatibility, and adjustable composition, CDots exhibit great potential in various applications such as catalysis, nanoprobe, optoelectronic devices, bioimaging, and biomedicine.<sup>20–25</sup> The first discovery of carbon-based fluorescent nanomaterials was in 2004, when Xu *et al.* synthesized single-walled carbon nanotubes *via* an electrophoretic and purification process using arc soot as a raw material. Surprisingly, fluorescent carbon was found separate from the mixture of reactants.<sup>26</sup> The first report of CDots as a carbon-based fluorescent nanomaterial was in 2006, when Sun *et al.* synthesized quantum-sized CDots through the laser ablation of a carbon target in the presence of water vapor using argon as a carrier gas. As the excitation wavelength increased, the emission wavelength of the CDots showed a continuous red shift.<sup>27</sup> Since then, CDot research and reports have expanded rapidly. In 2012, Wei *et al.* showed the possibility and importance of CDots as energy donors to build FRET systems for the first time. The fluorescence of CDots can be quenched by graphene *via* the FRET process and then restored upon the introduction of K<sup>+</sup>.<sup>28</sup> In 2013, Tang *et al.* reported an efficient CDot-based FRET system for the real-time monitoring of drug delivery and bioimaging. In this system, CDots served as both a FRET donor and a drug carrier, and doxorubicin served as an acceptor.<sup>9</sup> In 2016, Yu *et al.* reported FRET between CDots and rhodamine B based on an up-conversion process spanning three components, resulting in the efficient utilization of the apparently wasted portion of sunlight (200–800 nm).<sup>29</sup> In 2019, Su *et al.* described a straightforward strategy for preparing nanocomposites *via* the co-assembly of CDots and boron dipyrromethene based on FRET. The nanocomposite exhibited high water solubility, good biocompatibility, and photodynamic therapy efficiency.<sup>30</sup>

Many research efforts have attempted to build Cdot-based FRET systems as nanoprobe. Fig. 1 shows a timeline highlighting recent research efforts on Cdot-based FRET systems.<sup>8–16</sup> Many fluorescent molecules can be employed to construct FRET systems with CDots. Generally, a FRET system contains two kinds of fluorescent molecules with different emission wavelengths. When CDots act as donors, they transfer energy to another molecule to construct the FRET system. Conversely, when the CDots act as receptors, they accept energy from other molecules, achieving ratiometric luminescence *via* FRET. Previous reports demonstrate that paired CDot-based FRET systems exhibit high sensitivity and have been widely utilized in all fluorescence-based applications, including medical diagnosis, biological analysis, and optical imaging. As CDots and FRET have been detailed in many excellent reviews, this review focuses on Cdot-based FRET systems with respect to their construction strategies, beneficial properties, and potential in a variety of applications.

In this review, we present details on several Cdot-based FRET systems co-assembled from different classes of fluorescent materials, including organic fluorescent molecules, drug molecules, metal complexes, and nanomaterials. Based on the different fluorescent molecules, different combinations can be used to construct hetero-interfaces with CDots. These hetero-interfaces



**Biao Kong**

*Dr Biao Kong is currently a professor and National Thousand Youth Talents Plan fellow at Fudan University. He completed PhD degrees from Monash University (Australia) and Fudan University (China) under the supervision of Prof. Dongyuan Zhao and Selomulya Cordelia in 2015. He then served as a Research Fellow at the University of Melbourne (Australia) in 2015 and a Post-doctoral Fellow at Stanford University (USA) in 2016. Subsequently, he*

*was appointed as a professor of Global Expert of Thousand Talents Plan at Fudan University. His scientific interests focus on the rational design and fabrication of super-assembled framework-based soft hetero-interfaces and integrated devices for energy, catalysis, and biological applications.*

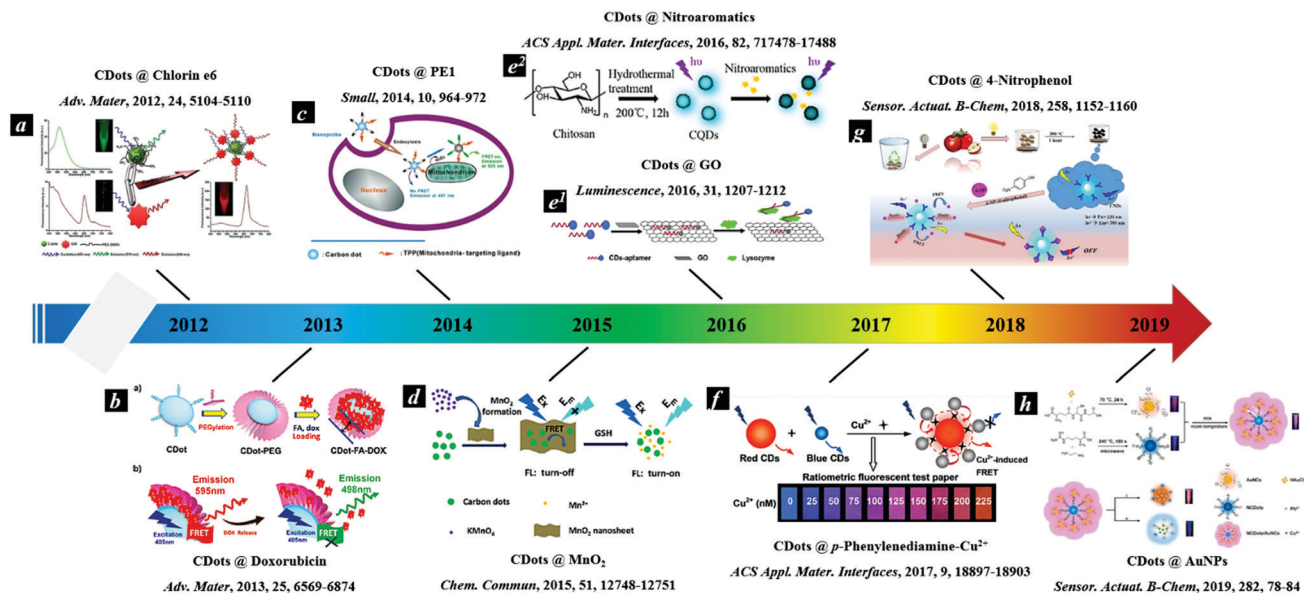


Fig. 1 Timeline showing recent studies on CDot-based FRET systems.<sup>8–16</sup> Reprinted with permission ref. 9–17. Copyright 2012 Wiley, Copyright 2013 Wiley, Copyright 2014 Wiley, Copyright 2015 The Royal Society of Chemistry, Copyright 2016 John Wiley and Sons Ltd, Copyright 2016 American Chemical Society, Copyright 2017 American Chemical Society, Copyright 2018 Elsevier, Copyright 2019 Elsevier.

are mainly based on covalent binding and surface functionalization/coupling, thus resulting in different FRET effects. We also review the synthetic strategies for CDot-based FRET systems and the applications of these systems in nanoprobe, bioimaging, and biomedicine.

## 2. Nanoprobes based on CDots and fluorescent molecules

### 2.1 CDots & fluorescent molecules

Fluorescent molecules exhibit characteristic fluorescence in the ultraviolet–visible–near-infrared region, and their fluorescence properties (excitation and emission wavelengths, intensity, lifetime, polarization, *etc.*) can be sensitively changed based on the properties of the environment (*e.g.*, polarity, refractive index, and viscosity). Based on the excellent and diverse properties of fluorescent molecules, many promising applications have been demonstrated. Unsurprisingly, many studies have focused on FRET between CDots and fluorescent molecules. Table 1 presents a survey of recent works on FRET systems based on fluorescent molecules and CDots along with their applications.

In 2012, Huang *et al.* reported a CDot–chlorin e6 FRET system based on a theranostic platform. Fig. 2a shows the FRET process between the CDots and chlorin Ce6, which combined through covalent binding. FRET occurs from the CDots to chlorin e6, and the CDots and CDots–chlorin e6 displayed green and red fluorescence, respectively. The CDots–Ce6 FRET system shows promise for applications in near-infrared fluorescence imaging-guided photodynamic therapy due to its excellent imaging and tumor-homing properties.<sup>8</sup> In 2013, Du *et al.* synthesized a ratiometric fluorescent nanoprobe with low cytotoxicity and high reversibility based on FRET for pH sensing (Fig. 2b).

In this nanoprobe, fluorescein isothiocyanate was assembled onto the CDots, which acted as the energy-transfer donor and carrier. The nanoprobe was successfully used to image live cells and reveal intracellular pH gradients.<sup>33</sup> In 2014, Du *et al.* reported a FRET-based ratiometric nanoprobe for mitochondrial H<sub>2</sub>O<sub>2</sub> in living cells (Fig. 2c). The FRET from the CDots (donor) to boronate-protected fluorescein (PF1; acceptor), which is covalently linked to the CDots, results in the blue emission of the CDots. As H<sub>2</sub>O<sub>2</sub> is added, FRET occurs between the CDots and PF1, resulting in green fluorescence. The ratiometric detection of H<sub>2</sub>O<sub>2</sub> is realized.<sup>10</sup> In 2018, Chatzimarkou *et al.* synthesized a sensitive and selective FRET-based nanoprobe for 4-nitrophenol (Fig. 2d). The synthesized N-CDots exhibited blue fluorescence, which can effectively be quenched by 4-nitrophenol through the FRET process from CDots to 4-nitrophenol. The CDots/4-nitrophenol showed bright luminescence and low toxicity, demonstrating promise for cell imaging and other biosensing applications.<sup>15</sup>

### 2.2 CDots & drug molecules

Drug molecules play a vital role in processes related to human health, such as nucleic acid repair, cell apoptosis, and tumor suppression. When coupled with CDots, certain drugs can be utilized to construct CDot–drug FRET systems, which show promising applications in nanoprobe, bioimaging, and biomedicine. Drug molecules commonly used in FRET include doxorubicin,<sup>9,56,57</sup> porphyrins,<sup>58,59</sup> vitamins,<sup>53,55,60</sup> curcumin,<sup>61</sup> rhodizonate,<sup>62</sup> and cisplatin(IV) prodrug.<sup>54</sup>

In 2013, Tang *et al.* reported an efficient CDot-based FRET system for the real-time monitoring of drug delivery and bioimaging. Fig. 3a shows the assembly process of a FRET–CDots drug delivery system (DDS) *via* direct surface coupling and the proposed mechanism of the FRET–CDots DDS for drug delivery. In this system, the CDots serve as both a donor and a

**Table 1** Representative examples of FRET systems based on fluorescent molecules and CDots along with their applications

Coupling molecule	Application	Ref.	Coupling molecule	Application	Ref.
Chlorin e6	Bioimaging, biomedicine	8	Naphthalimide	H <sub>2</sub> S nanoprobe	31
Naphthalimide	NO nanoprobe	32	Isothiocyanate	PH nanoprobe	33
NBD-PE; BODIPY-PH	Bioimaging	34	Rhodamine B	Fe <sup>3+</sup> nanoprobe	35
Boronate protected fluorescein (PFL)	H <sub>2</sub> O <sub>2</sub> nanoprobe, bioimaging	10	Trinitrophenol	Bioimaging	36
Nitroaromatics	Nanosensor	13	NBD-PE	Nanoprobe, bioimaging	37
Rhodamine B	Up-conversion properties	29	Chlorin e6	Bioimaging	38
Rhodamine 6G	Fe <sup>3+</sup> nanoprobe	39	TNB	DDVP nanoprobe	40
Naphthalimide	Nanoprobe, bioimaging	41	Ethidium bromide	DNA nanosensor	42
Glyphosate	Gly nanoprobe	43	2,3-Diaminophenazine	I <sup>-</sup> nanoprobe	44
Fluorescein	NH <sub>3</sub> nanoprobe	45	Isothiocyanate	PH nanoprobe	46
Acridone derivate	RNA nanoprobe	47	Naphthalimide	Tyrosinase nanoprobe	48
Rhodamine123	Bioimaging	49	Nitrophenol	Nanoprobe, bioimaging	15
Acriflavine	SEB nanoprobe	50	Fluorescein (FAM)	Zn <sup>+</sup> nanoprobe, bioimaging	51
Boron dipyrromethene	Bioimaging	30	Naphthalimide	Cys nanoprobe, bioimaging	52

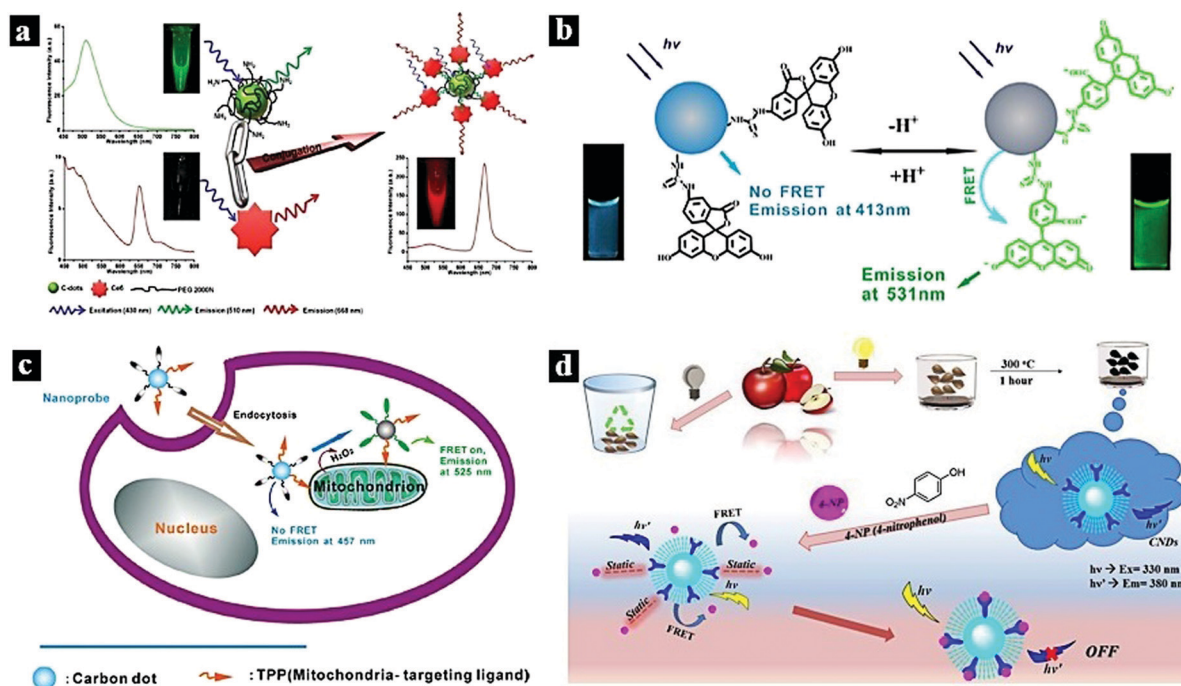


**Fig. 2** (a) FRET process between CDots and chlorin e6.<sup>8</sup> Reprinted with permission ref. 8. Copyright 2012 Wiley. (b) Schematic illustration of a Cdote-based FRET nanoprobe for pH sensing.<sup>33</sup> Reprinted with permission ref. 33. Copyright 2013 IOP Publishing Ltd. (c) Nanoprobe using FRET-based H<sub>2</sub>O<sub>2</sub> ratiometric sensing in a living cell.<sup>10</sup> Reprinted with permission ref. 10. Copyright 2014 Wiley-VCH Verlag. (d) Schematic illustration of the synthetic process of CDots and the FRET process between CDots and 4-nitrophenol.<sup>15</sup> Reprinted with permission ref. 15. Copyright 2018 Elsevier.

drug carrier, and doxorubicin serves as an acceptor. As doxorubicin is released from the surfaces of the CDots, the FRET between doxorubicin and the CDots is terminated, restoring the fluorescence of the CDots.<sup>9</sup> In 2015, Wang *et al.* reported a Cdote-based FRET system with high quantum yield (QY) for the detection of biologically significant vitamin B<sub>12</sub>. Fig. 3b shows the thermal reduction process of the high-QY CDots and the FRET process between the CDots and vitamin B<sub>12</sub>. The low-QY CDots exhibited emission wavelengths at 445 nm; after thermal treatment, the CDots showed high QY with an emission wavelength of 431 nm. The CDots were used to detect vitamin B<sub>12</sub> based on the FRET between the CDots and vitamin B<sub>12</sub>.<sup>53</sup> In 2017, Feng *et al.* reported a Cdote-based system for the real-time ratiometric monitoring of anticancer prodrug activation in living cells.

Fig. 3c shows the FRET process between the CDots and cisplatin(IV) prodrug. The quencher unit attached to the CDot surfaces through amide condensation. The CDots showed blue, green, and red emission under different excitation conditions as a drug nanocarrier. Based on the FRET between the CDots and cisplatin(IV) prodrug, the blue emission of the CDots was quenched. Under reductive conditions, the nanocarrier released the dabsyl unit and active Pt(II), causing the blue emission of the CDots to recover with time; meanwhile, the intensity of green and red fluorescence remained almost unchanged.<sup>54</sup> In 2015, Wang *et al.* reported a ratiometric fluorescent nanoprobe based on a N,S-CDots FRET system that was used for the determination of eriboflavin in aqueous solutions (Fig. 3d). The N,S-CDots exhibited blue emission at

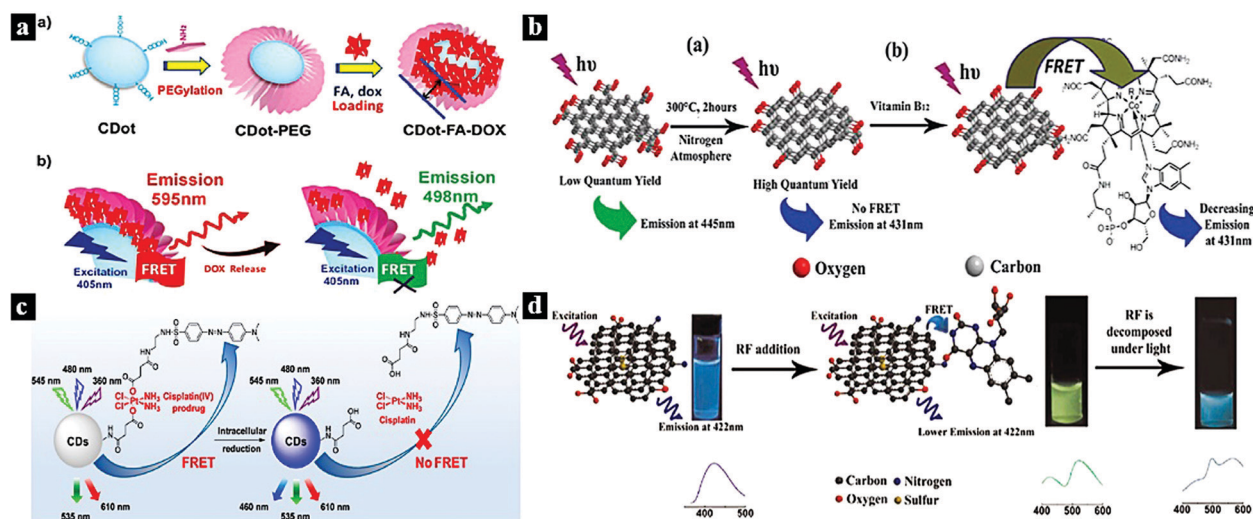


**Fig. 3** (a) Assembly process of FRET-CDots-DOX and the proposed mechanism of FRET-CDots-DOX for drug delivery.<sup>9</sup> Reprinted with permission ref. 9. Copyright 2013 Wiley. (b) Thermal reduction of high-QY CDots and the FRET process between CDots and vitamin B<sub>12</sub>.<sup>53</sup> Reprinted with permission ref. 53. Copyright 2015 The Royal Society of Chemistry. (c) FRET process between CDots and cisplatin(IV) prodrug.<sup>54</sup> Reprinted with permission ref. 54. Copyright 2017 American Chemical Society. (d) Schematic diagram of a riboflavin probe based on N,S-CDots and the FRET process.<sup>55</sup> Reprinted with permission ref. 55. Copyright 2015 Elsevier.

465 nm; through the FRET process from N,S-CDots to riboflavin, the blue emission intensity decreased monotonically, while the green emission intensity increased.<sup>55</sup>

### 2.3 CDots & metal complexes

The monitoring of metal ions is meaningful in the fields of human health and environmental protection. FRET systems based on CDot-metal complexes can act as efficient and sensitive nanoprobes for the detection of certain metal ions. The most investigated metal complexes include rhodamine-Al<sup>3+</sup>,<sup>63</sup> cobalt oxyhydroxide,<sup>64,65</sup> quercetin-Zn<sup>2+</sup>,<sup>66</sup> cyclam-Cu<sup>2+</sup>,<sup>67</sup> *p*-phenylenediamine-Cu<sup>2+</sup>,<sup>14</sup> ruthenium complex,<sup>68</sup> and HCM-Cu<sup>2+</sup>.<sup>69</sup>

In 2015, Kim *et al.* designed a CDot-rhodamine-Al<sup>3+</sup> FRET-based nanoprobe for Al<sup>3+</sup> detection in aqueous solution. Fig. 4a schematically illustrates the FRET process between the CDots and rhodamine-Al<sup>3+</sup>, which are covalently combined. The CDots act as an energy donor, while rhodamine-Al<sup>3+</sup> serves as an energy acceptor in the presence of Al<sup>3+</sup> ions. The emission of the CDots can be tuned from blue to green based on the FRET process from the CDots to rhodamine-Al<sup>3+</sup>.<sup>63</sup> In 2017, Liu *et al.* synthesized dual optical CDots-based ratiometric fluorescent nanoprobe for Cu<sup>2+</sup>. Fig. 4b schematically illustrates the FRET process from the blue CDots to the *p*-phenylenediamine-Cu<sup>2+</sup> complex. As Cu<sup>2+</sup> can coordinate with -COOH and *p*-phenylenediamine, this led to blue CDots joining to the surface of red CDots. FRET occurred from the blue CDots to *p*-phenylenediamine-Cu<sup>2+</sup> on the surfaces of the red CDots, leading to the fluorescence quenching of the blue CDots. The emission color could be tuned from blue to red based on the FRET process by adjusting the Cu<sup>2+</sup> doping content.<sup>14</sup> In 2015, Yang *et al.* reported fluorescent CDots as a sensitive nanoprobe for Zn<sup>2+</sup>. Fig. 4c schematically illustrates the detection of Zn<sup>2+</sup> based on a FRET system comprising CDots

and pentahydroxyflavone-Zn<sup>2+</sup> complex. Upon excitation at 360 nm, FRET occurred from the CDots to pentahydroxyflavone-Zn<sup>2+</sup>, while pentahydroxyflavone-Zn<sup>2+</sup> accepted the energy and exhibited fluorescence emission at 480 nm.<sup>66</sup> In 2018, Yan *et al.* reported a FRET-based ratiometric fluorescent nanoprobe for Cu<sup>2+</sup> using 7-diethylaminocoumarin-3-carbohydrazide (CMH)-functionalized CDots (Fig. 4d). In this system, CMH is covalently bound to the surfaces of the CDots, and FRET occurs from the CDots to CMH. However, the FRET process was inhibited by adding Cu<sup>2+</sup>; meanwhile, the fluorescence intensity increased at 400 nm and decreased at 458 nm. The emission can be tuned from blue to blue-green in the presence and absence of Cu<sup>2+</sup> under UV light.<sup>69</sup>

### 2.4 CDots & biomolecules

Biomolecules are an important part of higher flora and fauna due to their indispensable functions, such as helping cells transmit signals and controlling physiological and pathological processes. The biomolecules commonly applied in FRET include nucleic acids,<sup>70</sup> tryptophan,<sup>71</sup> and dopamine.<sup>72</sup>

In 2017, Khakbaz *et al.* reported a nanoprobe for micro-RNA sensing based on a FRET system. The FRET occurs between CDots and carboxyfluorescein-labeled DNA, and the CDot fluorescence is quenched. The nanoprobe can be used for micro-RNA detection and the early detection of breast cancer.<sup>70</sup> In 2017, Dang *et al.* synthesized a CDot-based FRET system *via* a one-step method using tryptophan and  $\beta$ -cyclodextrin as precursors. FRET was found to occur between tryptophan and the CDots, and this system could be used as a sensitive probe for Fe<sup>3+</sup> detection.<sup>71</sup> In 2017, Zhang *et al.* reported a FRET system based on polymerized dopamine (PDA) and CDots for bioimaging (Fig. 5). The FRET effect occurs between the CDots and PDA, resulting in highly efficient and tunable emission. The cell imaging ability and cytotoxicity of the CDot-PDA system were also explored, indicating

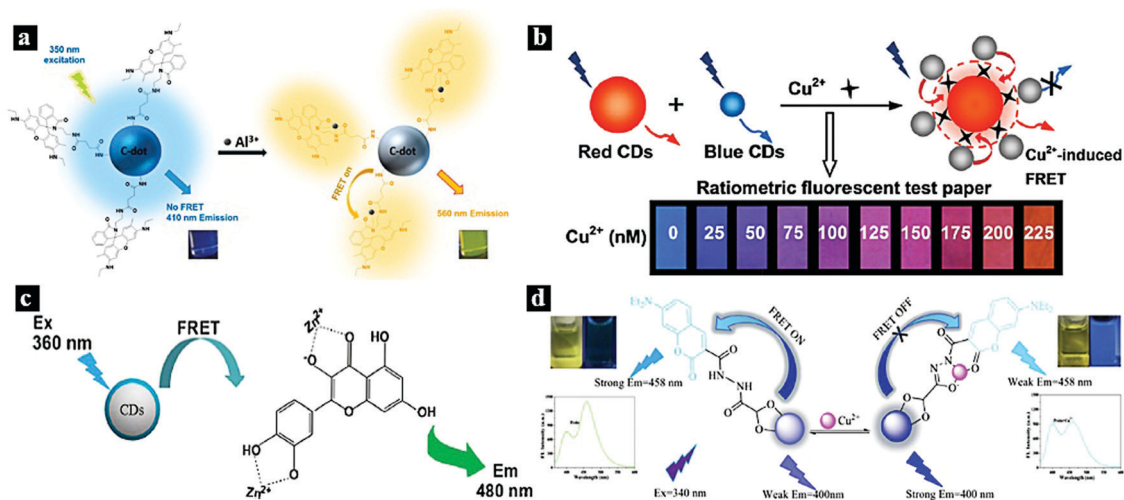


Fig. 4 (a) Schematic illustration of the FRET process between CDots and rhodamine–Al<sup>3+</sup>.<sup>63</sup> Reprinted with permission ref. 63. Copyright 2015 American Chemical Society. (b) Schematic illustration of the FRET process from blue CDots to *p*-phenylenediamine–Cu<sup>2+</sup>.<sup>14</sup> Reprinted with permission ref. 14. Copyright 2017 American Chemical Society. (c) Schematic illustration of the detection of Zn<sup>2+</sup> based on a CDots/pentahydroxyflavone–Zn<sup>2+</sup> FRET system.<sup>66</sup> Reprinted with permission ref. 64. Copyright 2015 Springer-Verlag Wien. (d) Schematic illustration of a FRET system based on CDots and CMH–Cu<sup>2+</sup>.<sup>69</sup> Reprinted with permission ref. 65. Copyright 2018 Elsevier.

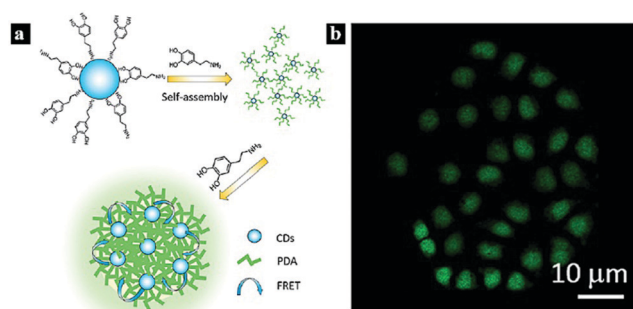


Fig. 5 (a) Schematic illustration of a nanoprobe based on FRET between CDots and PDA. (b) Confocal fluorescence images of MCF-7 cells under 405 nm laser excitation. Reprinted with permission ref. 76. Copyright 2017 The Royal Society of Chemistry.

good biocompatibility and strong prospects for biotechnological applications.<sup>72</sup>

### 3. Nanoprobes based on CDots and nanomaterials

#### 3.1 CDots & MnO<sub>2</sub>/MoS<sub>2</sub>

Layered transition-metal disulphides or dioxides (*e.g.*, MnO<sub>2</sub>, WS<sub>2</sub>, and MoS<sub>2</sub>) are a class of two-dimensional nanomaterials that show excellent properties, including large surface areas along with semiconducting and energy-harvesting characteristics, giving them widespread applications. Because of their excellent optical absorption capability and fast electron transfer rate, these materials are promising fluorescence quenchers and have attracted considerable attention in the construction of FRET-based sensing platforms.

MnO<sub>2</sub> is one of the most stable manganese oxides and possesses excellent chemical and physical properties. As a transition metal

oxide, it attracts considerable attention in batteries, supercapacitors, and even catalysis driven by visible light. MnO<sub>2</sub> shows broad absorption in the range of 250–550 nm, which overlaps with the fluorescence excitation of CDots. This phenomenon allows the occurrence of FRET between CDots and MnO<sub>2</sub>.<sup>11,73–79</sup> The transition metal oxide MoS<sub>2</sub> has a sandwich structure that is bonded by weak van der Waals forces and can be regarded as S–Mo–S. MoS<sub>2</sub> possesses a large intrinsic band gap that depends largely on the number of layers. In addition, most transition metal ions have inherent fluorescence quenching characteristics. Therefore, many FRET systems based on CDots and MoS<sub>2</sub> have been reported.<sup>80–83</sup>

In 2015, Wang *et al.* reported a FRET system between CDots and MnO<sub>2</sub> for glutathione (GSH) sensing in human whole blood samples (Fig. 6a). Due to the FRET from the CDots to MnO<sub>2</sub> through MnO<sub>2</sub>-surface functionalization with CDots, the fluorescence emission of the CDots was quenched. After the introduction of GSH, the fluorescence of the CDots was restored.<sup>11</sup> In 2018, Yan *et al.* synthesized a CDots–MnO<sub>2</sub> FRET platform and applied it in the sensitive detection of organophosphorus pesticides (Fig. 6b). The fluorescence intensity of the CDots can be tuned off *via* FRET from CDots to the energy acceptor MnO<sub>2</sub>. Moreover, the quenching effect induced by MnO<sub>2</sub> nanosheets can be restored by adding acetylthiocholine and butyrylcholinesterase to the FRET system.<sup>74</sup> In 2015, Yang *et al.* reported a turn-on fluorescence nanoprobe for GSH in aqueous solutions based on a CDots–MnO<sub>2</sub> FRET system (Fig. 6c). The CDots–MnO<sub>2</sub> complex is easily synthesized *via* surface functionalization and exhibits a stable FRET process. The MnO can be reduced in the presence of GSH introduced into the system, thereby inhibiting the FRET process between the CDots and MnO<sub>2</sub> and restoring the fluorescence intensity.<sup>75</sup> In 2017, Jana *et al.* reported a CDots–MnO<sub>2</sub> FRET system for molecular logic operations using *N*-acetyl-L-cysteine (NAC) and H<sup>+</sup> as inputs (Fig. 6d). The FRET process occurs from the CDots to

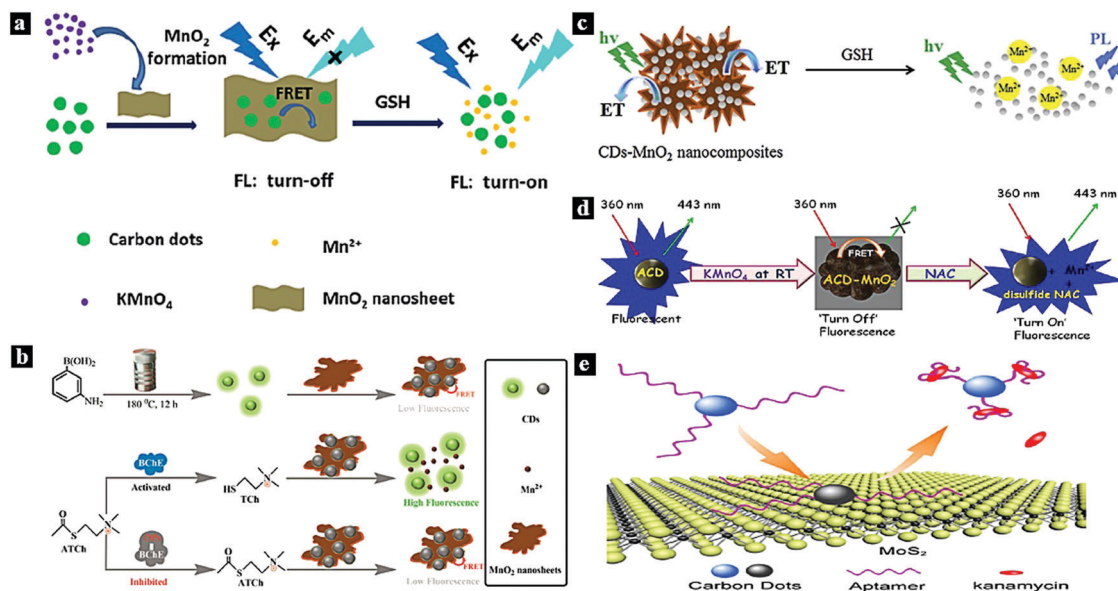


**Fig. 6** (a) Schematic illustration of the preparation of a nanoprobes for GSH based on a CDots-MnO<sub>2</sub> FRET system.<sup>11</sup> Reprinted with permission ref. 11. Copyright 2015 The Royal Society of Chemistry. (b) Schematic illustration of a nanoprobes for organophosphorus pesticides based on a CDots-MnO<sub>2</sub> FRET system.<sup>74</sup> Reprinted with permission ref. 70. Copyright 2018 American Chemical Society. (c) Schematic illustration of a nanoprobes for organophosphorus pesticides based on a CDots-MnO<sub>2</sub> FRET system.<sup>75</sup> Reprinted with permission ref. 71. Copyright 2015 Elsevier. (d) Schematic illustration of an NAC nanoprobes for organophosphorus pesticides based on a FRET system.<sup>77</sup> (e) Schematic illustration of a kanamycin sensing strategy based on a CDots-MoS<sub>2</sub> FRET system.<sup>81</sup> Reprinted with permission ref. 73. Copyright 2017 Springer-Verlag Wien.

MnO<sub>2</sub>, resulting in fluorescence quenching; the fluorescence can be restored by adding NAC.<sup>77</sup> In 2017, Wang *et al.* synthesized a CDots-MoS<sub>2</sub> FRET platform and used it for the sensitive detection of the antibiotic kanamycin (Fig. 6e). Through van der Waals forces, the CDots can be assembled onto the MoS<sub>2</sub> surface, thus quenching the fluorescence due to the FRET from the CDots to MoS<sub>2</sub>.<sup>81</sup>

### 3.2 CDots & Au/Ag

Metal nanoparticles and particularly Ag and Au have attracted great research interest due to their physicochemical and photoelectric properties. Therefore, they are widely used in catalytic, photovoltaic, and biological applications. Au and Ag nanoparticles (AuNPs and AgNPs) can also be used as efficient acceptors for most fluorescent groups due to their high extinction coefficients and absorption bandwidths. Therefore, AuNPs<sup>89–95</sup> and AgNPs<sup>96–100</sup> are ideal nano-quenching agents to establish FRET-based nanoprobes due to their large extinction coefficients and wide absorption spectra, which overlap with the fluorescent emission of CDots.

In 2017, Shen *et al.* synthesized a fluorescent nanoprobes for the sensitive detection of adenosine based on FRET. Fig. 7a schematically illustrates the nanoprobes for adenosine based on FRET between CDots and AuNPs. Through the hybridization between single-strand DNA (ssDNA)-functionalized CDots and aptamer-functionalized AuNPs, fluorescence quenching was observed due to FRET from the CDots to the AuNPs. When adenosine was present, the binding between adenosine and aptamer released the ssDNA-functionalized CDots from the AuNP surfaces, resulting in fluorescence recovery.<sup>84</sup> In 2017,

Li *et al.* reported a CDots-Au nanocluster FRET system combined *via* a carbodiimide-activated coupling reaction as a ratiometric fluorescence nanoprobes for the bioimaging of H<sub>2</sub>O<sub>2</sub> (Fig. 7b). The synthesized CDots-Au system showed a dual-emission fluorescent property with 40% FRET efficiency from the CDots to Au. Furthermore, the red emission of the CDots-Au system could be quenched by H<sub>2</sub>O<sub>2</sub>, while the blue emission was used as a reference signal to provide built-in correction.<sup>85</sup> In 2018, Ge *et al.* synthesized a selective and sensitive nanoprobes for the antibiotic D-penicillamine (D-PA) based on a FRET system between CDots and AuNPs combined *via* electrostatic interaction (Fig. 7c). In this system, AuNPs act as a colorimetric indicator and a fluorescence quencher. The CDot fluorescence can be quenched through the FRET process from the CDots to the AuNPs. Moreover, the quenching effect induced by the AuNPs can be restored by adding acetylthiocholine and D-PA to the FRET system.<sup>86</sup> In 2019, Wang *et al.* synthesized a CDots-AuNCs FRET-based ratiometric fluorescent nanoprobes for Pb<sup>2+</sup>/Cu<sup>2+</sup> (Fig. 7d). The probe was simply prepared by mixing AuNCs and N-CDots in aqueous solution. The probe can interact selectively with Pb<sup>2+</sup> and Cu<sup>2+</sup>, leading to a shift in the fluorescent signal. The system showed good detection sensitivity at 0.5 and 0.15 μM for Pb<sup>2+</sup> and Cu<sup>2+</sup>, respectively.<sup>16</sup> In 2018, He *et al.* reported a CDots-AuNCs FRET-based dual-emission ratiometric fluorescence nanoprobes for dopamine sensing (Fig. 7e). The FRET-based nanoprobes consists of two fluorophores (AuNCs as the acceptor and CDots as the energy donor) and exhibits dual emission wavelengths of 610 and 420 nm under excitation at 380 nm. The AuNCs were subsequently conjugated to the CDots *via* simple surface functionalization.

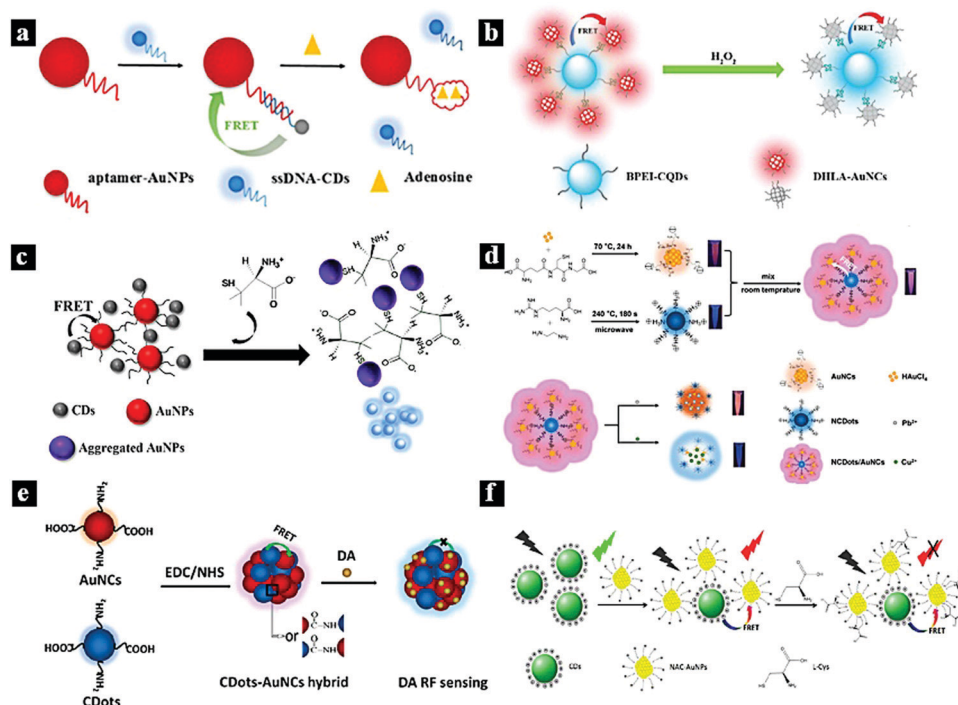


**Fig. 7** (a) Schematic illustration of a nanoprobe for adenosine based on FRET between CDots and AuNPs.<sup>84</sup> Reprinted with permission ref. 84. Copyright 2017 The Royal Society of Chemistry. (b) Schematic illustration of a FRET-based nanoprobe for  $\text{H}_2\text{O}_2$ .<sup>85</sup> Reprinted with permission ref. 85. Copyright 2017 Elsevier. (c) Schematic illustration of a FRET-based nanoprobe for  $\text{D-PA}$ .<sup>86</sup> Reprinted with permission ref. 86. Copyright 2018 Springer New York. (d) Schematic illustration of a ratiometric nanoprobe for  $\text{Pb}^{2+}/\text{Cu}^{2+}$  based on a CDots–Au FRET system.<sup>16</sup> Reprinted with permission ref. 16. Copyright 2019 Elsevier. (e) Schematic illustration of a dopamine nanoprobe based on a CDots–Au FRET system.<sup>87</sup> Reprinted with permission ref. 87. Copyright 2018 Elsevier. (f) Schematic illustration of a nanoprobe for  $\text{L-cysteine}$  based on a FRET system between CDots and AuNPs.<sup>88</sup> Reprinted with permission ref. 88. Copyright 2019 Elsevier.

The fluorescence of the AuNCs can be quenched by dopamine, inhibiting the FRET process from the CDots to Au.<sup>87</sup> In 2019, Dong *et al.* reported a nanoprobe for the ratiometric detection of  $\text{L-cysteine}$  based on FRET between CDots and AuNPs (Fig. 7f). FRET was established from the energy donor (CDots) to the acceptor (AuNPs), which were combined *via* electrostatic interaction, effectively inhibiting the fluorescence emission of the CDots. After the addition of  $\text{L-cysteine}$  to the system, the fluorescence of the NAC-AuNPs was quenched, while the emission intensity of the CDots remained almost constant.<sup>88</sup>

### 3.3 CDots & graphene oxide

Graphene oxide (GO) is a two-dimensional graphitic carbon system with monoatomic thickness and oxygen-containing functional groups. Due to its good water solubility, large specific surface area, high electronic conductivity, and long-range nanoscale energy transfer characteristics, GO has attracted significant research attention. Recently, it has been used as a good energy acceptor to quench the fluorescence of CDots based on the FRET process.<sup>12,28,101–104</sup>

In 2012, Wei *et al.* reported a metal-ion nanoprobe with high selectivity and tunable dynamic range based on FRET from CDots to GO. Fig. 8a shows a schematic illustration of the nanoprobe for  $\text{K}^+$  sensing based on the CDots–GO FRET system, in which the CDots and GO are combined *via* a specific cation–ligand complexation reaction. The fluorescence of the

CDots can be quenched by GO based on the FRET process; however, after the introduction of  $\text{K}^+$ , which competes with ammonium functionalized on GO, the fluorescence of the CDots was restored.<sup>28</sup> In 2016, Wu *et al.* synthesized a photoluminescent nanoprobe for the detection of lysozyme based on FRET from CDots to GO (Fig. 8b). Upon the addition of GO, the photoluminescence of the aptamer-conjugated CDots was effectively quenched because of the FRET from CDots to GO. However, in the presence of the target lysozyme, the CDots bound strongly to lysozyme *via* the aptamer–lysozyme interaction and desorbed from the GO surface, causing the photoluminescence of the CDots to recover.<sup>12</sup> In 2015, Cui *et al.* synthesized a fluorescent nanoprobe for  $\text{Hg}^{2+}$  detection based on FRET between CDots and graphene oxide (Fig. 8c). The fluorescent signal of the CDots was quenched upon binding to GO based on the FRET process. However, when  $\text{Hg}^{2+}$  was present, oligodeoxyribonucleotide-functionalized CDots selectively bound to  $\text{Hg}^{2+}$  ions in solution and initiated the adsorption of CDots from GO, causing the CDot fluorescence to recover.<sup>101</sup> In 2018, Cheng *et al.* synthesized a fluorometric nanoprobe for adenosine triphosphate (ATP) sensing based on FRET between CDots and GO (Fig. 8d). The CDots and GO were combined through  $\pi$  stacking and hydrophobic interactions. CDots and GO acted as the energy donor and acceptor, respectively, resulting the quenching of the CDot fluorescence. When ATP was present, the aptamer bound strongly to ATP, causing

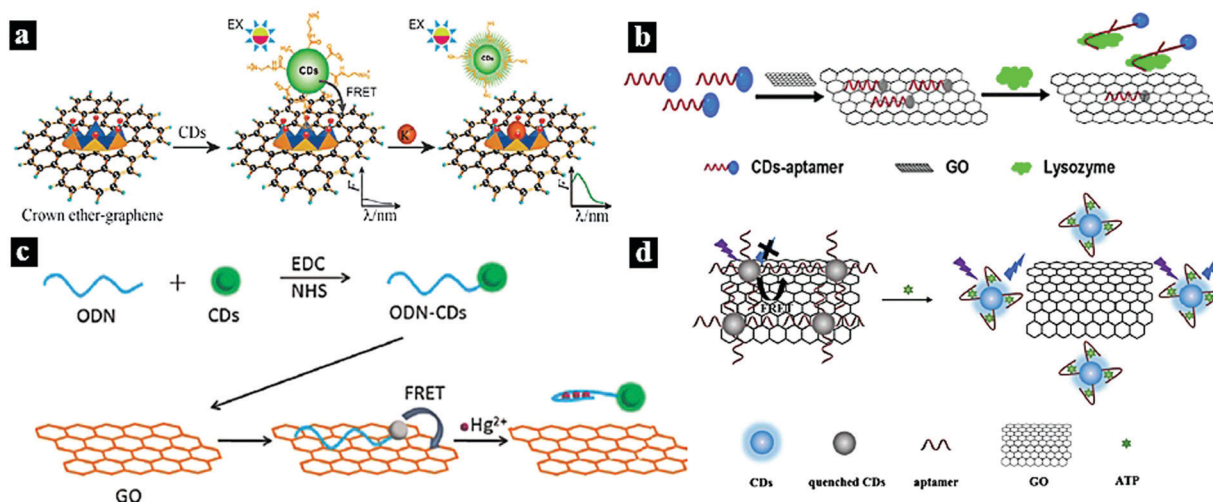


**Fig. 8** (a) Schematic illustration of a nanoprobe for K<sup>+</sup> based on a CDots–GO FRET system.<sup>28</sup> Reprinted with permission ref. 28. Copyright 2012 The Royal Society of Chemistry. (b) Schematic illustration of a nanoprobe for lysozyme based on a CDots–GO FRET system.<sup>12</sup> Reprinted with permission ref. 12. Copyright 2016 John Wiley and Sons Ltd. (c) Schematic illustration of a FRET system for Hg<sup>2+</sup> detection.<sup>101</sup> Reprinted with permission ref. 101. Copyright 2015 Elsevier Ltd. (d) Schematic illustration of a nanoprobe for ATP based on FRET between CDots and GO.<sup>102</sup> Reprinted with permission ref. 102. Copyright 2018 Springer-Verlag Wien.

the CDots to unbind from GO and the CDot fluorescence to recover.<sup>102</sup>

### 3.4 CDots & quantum dots

Fluorescence resonance energy transfer between CDots and quantum dots has also been widely studied. The main studied quantum dots include CdTe,<sup>105</sup> CDots,<sup>106</sup> graphene quantum dots.<sup>107</sup> In 2014, Tao *et al.* reported a nanoprobe for chlortoluron detection in water

based on a FRET system between CDots and CdTe quantum dots. The FRET occurs from the CDots (donor) to CdTe (acceptor), greatly enhancing the fluorescence intensity of CdTe. After the addition of chlortoluron, the strong interaction between CdTe and chlortoluron leads to the quenching of CdTe fluorescence by the formation of the chlortoluron–CdTe ground state complex.<sup>105</sup> In 2016, Wang *et al.* reported a nanoprobe for volatile organic compounds based on intra-particle FRET in Mn–CDots. The FRET occurs from the

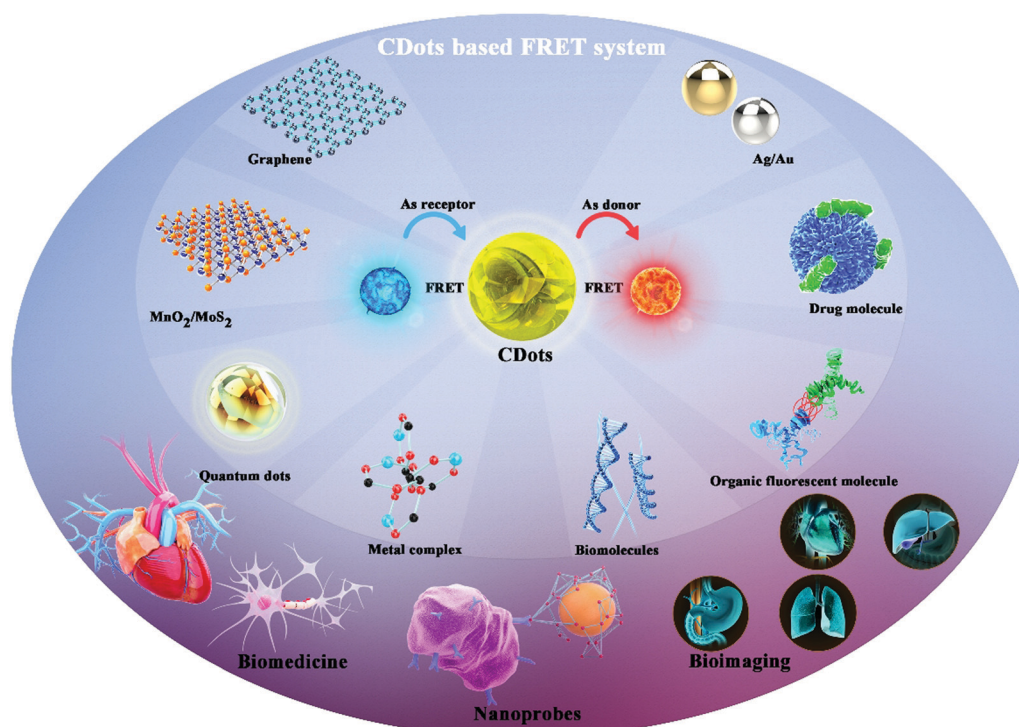


**Fig. 9** Perspectives for potential future applications of Cdot-based FRET systems.

surface-related energy donor to the metal-related energy acceptor in the Mn-CDots. The FRET is not sensitive to proximity; instead, it is sensitive to polarity resulting from the inherent fixed position of the two fluorescent groups on the CDot backbone. Therefore, based on the sensitivity of the FRET, the Mn-CDots have extraordinary sensing ability for some small molecules.<sup>106</sup> In 2019, Chini *et al.* reported a nanoprobe for sensing heavy metal ions based on a FRET system between CDots and graphene quantum dots. In this FRET system, the graphene quantum dots serve as the energy donor, while the CDots are the acceptor. After the addition of heavy metals such as mercury ( $\text{Hg}^{2+}$ ) and arsenic ( $\text{As}^{5+}$ ) into this nanoprobe system, the FRET signal was significantly reduced.<sup>107</sup>

## 4. Conclusions & perspectives

CDots have recently emerged as a new class of fluorescent carbon nanomaterials and gained tremendous attention due to their excellent physicochemical properties, which distinguish them from traditional fluorescent materials. The major advantages of CDot-based FRET systems include high sensitivity, adjustable composition, and good biocompatibility, which make them promising materials for nanoprobe, bioimaging, and biomedicine. In comparison with conventional FRET systems, CDot-based FRET systems overcome drawbacks such as spectral crosstalk, photobleaching, and direct acceptor excitation. CDot-based FRET systems also provide increased sensitivity, for single function and multifunction use. As a new type of nanomaterial with excellent optical properties, CDots can serve as an energy donor and receptor, greatly improving the application range and efficacy of CDot-based FRET systems. Perspectives for potential future applications of CDot-based FRET systems are summarized in Fig. 9.

Research on the design and fabrication of CDot-based FRET systems has become of great interest in chemical and biological sciences along with engineering fields. With the development of FRET-based nanoprobe, the functional units of FRET have been expanded from simple molecules to macromolecule and nanoparticles, and the research focus has shifted from single measurements to multifunctional and interdisciplinary applications. CDot-based FRET nanoprobe show promise for achieving high sensitivity, high selectivity, portability, fast response, and biocompatibility, which are important in applications in biotechnology, the environment, and medicine. For example, all-in-one diagnostic platforms for recognition, imaging, and therapy have received increasing attention. However, a great number of challenges and opportunities remain.<sup>108</sup> For example, while numerous optical light-emitting diode devices have been reported, further research in the field of biological devices is needed. This review summarized recent progress in the research and development of CDot-based FRET systems with a focus on the different classifications of fluorescent molecules and potential applications in nanoprobe. We reviewed several fluorescent molecules in detail, including organic fluorescent molecules, drug molecules, metal complexes, biomolecules,  $\text{MnO}_2/\text{MoS}_2$ , Au/Ag, graphene/GO, and quantum dots. We also

presented extensive applications of CDot-based FRET systems as highly sensitive nanoprobe for diverse analytes.

Although many applications of CDot-based FRET systems have been reported, challenges remain. First, for CDots acting as the energy donor, new energy receptors are needed to facilitate efficient energy transfer and increase detection sensitivity. Second, for CDots acting as the energy receptor, new energy donors should be explored. Thus, CDots can be enabled to exhibit superior optical performance for nanoprobe and biological applications. Third, novel CDots based on heteroatom doping and surface functionalization should be explored to allow the FRET process to be modulated by preparing CDots with different properties. In summary, exploring new energy transfer donor and receptor pairs for FRET systems is important to improve FRET efficiency and analytical performance. CDot-based FRET systems will undoubtedly overcome the limitations of traditional luminescent materials and have a bright future in nanoprobe, bioimaging, biomedicine and other applications.

## Conflicts of interest

There are no conflicts to declare.

## Acknowledgements

This work was supported by the National Key R&D Program of China (2017YFA0206901, 2017YFA0206900), the NSF of China (21705027), the Major Scientific and Technological Innovation Project of Shandong (2017CXGC0501), the Natural Science Foundation of Shandong Province (ZR2017PEM004, and ZR2017BEM020), the Recruitment Program of Global Experts of China and the Recruitment Program of Global Experts of Shanghai, and the Australia National Health and Medical Research Council (NHMRC APP1163786).

## References

- 1 A. T. Aron, M. O. Loehr, J. Bogena and C. J. Chang, *J. Am. Chem. Soc.*, 2016, **138**, 14338–14346.
- 2 R. Vafabakhsh, J. Levitz and E. Y. Isacoff, *Nature*, 2015, **524**, 497.
- 3 J. Guo, X. Qiu, C. Mingoies, J. R. Deschamps, K. Susumu, I. L. Medintz and N. Hildebrandt, *ACS Nano*, 2019, **13**, 505–514.
- 4 J. Liu and Y. Lu, *J. Am. Chem. Soc.*, 2002, **124**, 15208–15216.
- 5 E. Galperin, V. V. Verkhusha and A. Sorkin, *Nat. Methods*, 2004, **1**, 209–217.
- 6 Y. Yang, H. Liu, M. Han, B. Sun and J. Li, *Angew. Chem., Int. Ed.*, 2016, **55**, 13538–13543.
- 7 S. Basu, L.-M. Needham, D. Lando, E. J. R. Taylor, K. J. Wohlfahrt, D. Shah, W. Boucher, Y. L. Tan, L. E. Bates, O. Tkachenko, J. Cramard, B. C. Lagerholm, C. Eggeling, B. Hendrich, D. Klenerman, S. F. Lee and E. D. Laue, *Nat. Commun.*, 2018, **9**, 2520.

- 8 H. Peng, L. Jing, W. Xiansong, W. Zhe, Z. Chunlei, H. Meng, W. Kan, C. Feng, L. Zhiming and S. Guangxia, *Adv. Mater.*, 2012, **24**, 5104–5110.
- 9 T. Jing, K. Biao, W. Hao, X. Ming, W. Yongcheng, W. Yanli, Z. Dongyuan and Z. Gengfeng, *Adv. Mater.*, 2013, **25**, 6569–6574.
- 10 F. Du, Y. Min, F. Zeng, C. Yu and S. Wu, *Small*, 2014, **10**, 964–972.
- 11 W. Yuhui, J. Kai, Z. Jiali, Z. Ling and L. Hengwei, *Chem. Commun.*, 2015, **51**, 12748–12751.
- 12 J. Wu, Y. Hou, P. Wang, Z. Wang, Y. Li, S. Wang and M. Yang, *Luminescence*, 2016, **31**, 1207–1212.
- 13 Z. Liang, M. Kang, G. F. Payne, X. Wang and R. Sun, *ACS Appl. Mater. Interfaces*, 2016, **8**, 17478–17488.
- 14 C. Liu, D. Ning, C. Zhang, Z. Liu, R. Zhang, J. Zhao, T. Zhao, B. Liu and Z. Zhang, *ACS Appl. Mater. Interfaces*, 2017, **9**, 18897–18903.
- 15 A. Chatzimitakou, T. G. Chatzimitakos, A. Kasouni, L. Sygellou, A. Avgeropoulos and C. D. Stalikas, *Sens. Actuators, B*, 2018, **258**, 1152–1160.
- 16 L. Wang, H.-X. Cao, Y.-S. He, C.-G. Pan, T.-K. Sun, X.-Y. Zhang, C.-Y. Wang and G.-X. Liang, *Sens. Actuators, B*, 2019, **282**, 78–84.
- 17 G. Chen, F. Song, X. Xiong and X. Peng, *Ind. Eng. Chem. Res.*, 2013, **52**, 11228–11245.
- 18 B. Prevo and E. J. G. Peterman, *Chem. Soc. Rev.*, 2014, **43**, 1144–1155.
- 19 W. R. Algar, H. Kim, I. L. Medintz and N. Hildebrandt, *Coord. Chem. Rev.*, 2014, **263–264**, 65–85.
- 20 J. Tang, Y. Zhang, B. Kong, Y. Wang, P. Da, J. Li, A. A. Elzatahry, D. Zhao, X. Gong and G. Zheng, *Nano Lett.*, 2014, **14**, 2702–2708.
- 21 B. Kong, J. Tang, Y. Zhang, T. Jiang, X. Gong, C. Peng, J. Wei, J. Yang, Y. Wang, X. Wang, G. Zheng, C. Selomulya and D. Zhao, *Nat. Chem.*, 2015, **8**, 171.
- 22 S. Tao, S. Lu, Y. Geng, S. Zhu, S. A. T. Redfern, Y. Song, T. Feng, W. Xu and B. Yang, *Angew. Chem., Int. Ed.*, 2018, **57**, 2393–2398.
- 23 H. Li, Z. Kang, Y. Liu and S.-T. Lee, *J. Mater. Chem.*, 2012, **22**, 24230–24253.
- 24 L. Wang, X. Wu, S. Guo, M. Han, Y. Zhou, Y. Sun, H. Huang, Y. Liu and Z. Kang, *J. Mater. Chem. A*, 2017, **5**, 2717–2723.
- 25 B. Kong, A. Zhu, C. Ding, X. Zhao, B. Li and Y. Tian, *Adv. Mater.*, 2012, **24**, 5844–5848.
- 26 X. Xu, R. Ray, Y. Gu, H. J. Ploehn, L. Gearheart, K. Raker and W. A. Scrivens, *J. Am. Chem. Soc.*, 2004, **126**, 12736–12737.
- 27 Y.-P. Sun, B. Zhou, Y. Lin, W. Wang, K. A. S. Fernando, P. Pathak, M. J. Meziani, B. A. Harruff, X. Wang, H. Wang, P. G. Luo, H. Yang, M. E. Kose, B. Chen, L. M. Veca and S.-Y. Xie, *J. Am. Chem. Soc.*, 2006, **128**, 7756–7757.
- 28 W. Wei, C. Xu, J. Ren, B. Xu and X. Qu, *Chem. Commun.*, 2012, **48**, 1284–1286.
- 29 S. Yu, Y. L. Su, H. N. Umh and J. Yi, *Nano Energy*, 2016, **26**, 479–487.
- 30 Y. Su, S. Lu, P. Gao, M. Zheng and Z. Xie, *Mater. Chem. Front*, 2019, **3**, 1747–1753.
- 31 Y. Changmin, L. Xizhen, Z. Fang, Z. Fangyuan and W. Shuizhu, *Chem. Commun.*, 2013, **49**, 403–405.
- 32 C. Yu, Y. Wu, Z. Fang and S. Wu, *J. Mater. Chem. B*, 2013, **1**, 4152.
- 33 F. Du, Y. Ming, F. Zeng, C. Yu and S. Wu, *Nanotechnology*, 2013, **24**, 365101.
- 34 N. Sukhendu, M. Ravit, P. K. Kaviya, M. Yelena, K. Sofiya and J. Raz, *Chem. Commun.*, 2014, **50**, 10299–10302.
- 35 S. Hu, Q. Zhao, Q. Chang, J. Yang and J. Liu, *RSC Adv.*, 2014, **4**, 41069–41075.
- 36 D. Shi, F. Yan, T. Zheng, Y. Wang, X. Zhou and C. Li, *RSC Adv*, 2015, **5**, 98492–98499.
- 37 S. Nandi, R. Malishev, S. K. Bhunia, S. Kolusheva, J. Jopp and R. Jelinek, *Biophys. J.*, 2016, **110**, 2016–2025.
- 38 K. Yang, L. Fan, W. Y. Che, X. Hu and T. Feng, *RSC Adv.*, 2016, **6**, 101447–101451.
- 39 M. Deng, W. Sha, C. Liang, H. Shang and S. Jiang, *RSC Adv.*, 2016, **6**, 26936–26940.
- 40 J. Hou, Z. Tian, H. Xie, Q. Tian and S. Ai, *Sens. Actuators, B*, 2016, **232**, 477–483.
- 41 J. S. Sidhu, A. Singh, N. Garg and N. Singh, *ACS Appl. Mater. Interfaces*, 2017, **9**, 25847–25856.
- 42 J. Kudr, L. Richtera, K. Xhaxhiu, D. Hynek, Z. Heger, O. Zitka and V. Adam, *Biosens. Bioelectron.*, 2017, **92**, 133–139.
- 43 Y. Yuan, J. Jiang, S. Liu, J. Yang, Z. Hui, J. Yan and X. Hu, *Sens. Actuators, B*, 2017, **242**, 545–553.
- 44 H. Wang, Q. Lu, Y. Liu, H. Li, Y. Zhang and S. Yao, *Sens. Actuators, B*, 2017, **250**, 429–435.
- 45 H. Chao-Peng, H. Zahraasadat, A. Efe, Z. Shanyu, S. Michel, Z. Haijiang, G. Huizhang, W. Lukas, R. M. Rossi and M. M. Koebel, *Sens. Actuators, B*, 2017, **253**, 714–722.
- 46 H. Liu, C. Xu, Y. Bai, L. Liu, D. Liao, J. Liang, L. Liu and H. Han, *Spectrochim. Acta, Part A*, 2017, **171**, 311–316.
- 47 Y. Xia, L. Wang, J. Li, X. Chen and J. H. Chen, *Anal. Chem.*, 2018, **90**, 8969–8976.
- 48 J. S. Sidhu and N. Singh, *J. Mater. Chem. B*, 2018, **6**, 4139–4145.
- 49 A. Das, D. Roy, M. Mandal, C. Jaiswal, M. Ta and P. K. Mandal, *J. Phys. Chem. Lett.*, 2018, **9**, 5092–5099.
- 50 S. Kumari, M. Tiwari and P. Das, *Sens. Actuators, B*, 2019, **279**, 393–399.
- 51 Y. Shu, N. Zheng, A.-Q. Zheng, T.-T. Guo, Y.-L. Yu and J.-H. Wang, *Anal. Chem.*, 2019, **91**, 4157–4163.
- 52 J. S. Sidhu, A. Singh, N. Garg, N. Kaur and N. Singh, *Sens. Actuators, B*, 2019, **282**, 515–522.
- 53 J. Wang, J. Wei, S. Su and J. Qiu, *New J. Chem.*, 2015, **39**, 501–507.
- 54 T. Feng, H. J. Chua and Y. Zhao, *ACS Biomater. Sci. Eng.*, 2017, **3**, 1535–1541.
- 55 J. Wang, S. Su, J. Wei, R. Bahgi, L. Hope-Weeks, J. Qiu and S. Wang, *Physica E*, 2015, **72**, 17–24.
- 56 H. Chen, Z. Wang, S. Zong, P. Chen, D. Zhu, L. Wu and Y. Cui, *Nanoscale*, 2015, **7**, 15477–15486.
- 57 S. Liu, *IOP Conf. Ser.*, 2018, **382**, 022055.

- 58 F. Colin, N. Nikolitsa, A. P. Mchale, M. C. Bridgeen and J. F. Callan, *Chem. Commun.*, 2013, **49**, 8934–8936.
- 59 J. Wang, Z. Zhang, S. Zha, Y. Zhu, P. Wu, B. Ehrenberg and J. Y. Chen, *Biomaterials*, 2014, **35**, 9372–9381.
- 60 L. Lin, Y. Wang, Y. Xiao and X. Chen, *Anal. Bioanal. Chem.*, 2019, **411**, 2803–2808.
- 61 Y. Shi, C. Li, S. Liu, Z. Liu, J. Zhu, J. Yang and X. Hu, *RSC Adv*, 2015, **5**, 64790–64796.
- 62 M. Ganiga and J. Cyriac, *Sens. Actuators, B*, 2016, **225**, 522–528.
- 63 Y. Kim, G. Jang and T. S. Lee, *ACS Appl. Mater. Interfaces*, 2015, **7**, 15649–15657.
- 64 L. Linbo, W. Chao, L. Kangyu, W. Yuhuan, L. Kun and L. Yuqing, *Anal. Chem.*, 2015, **87**, 3404–3411.
- 65 G. Li, W. Kong, M. Zhao, S. Lu, P. Gong, G. Chen, L. Xia, H. Wang, J. You and Y. Wu, *Biosens. Bioelectron.*, 2016, **79**, 728–735.
- 66 M. Yang, W. Kong, L. Hao, J. Liu, H. Hui, L. Yang and Z. Kang, *Micro. Acta*, 2015, **182**, 2443–2450.
- 67 J. Chen, Y. Li, K. Lv, W. Zhong, H. Wang, Z. Wu, P. Yi and J. Jiang, *Sens. Actuators, B*, 2016, **224**, 298–306.
- 68 D. Yang, S. Guan, Y. Niu, Z. Xie, S. Zhou and X. Qu, *J. Mater. Chem. B*, 2018, **6**, 2315–2322.
- 69 F. Yan, Z. Bai, Y. Chen, F. Zu, X. Li, J. Xu and L. Chen, *Sens. Actuators, B*, 2018, **275**, 86–94.
- 70 F. Khakbaz and M. Mahani, *Anal. Biochem.*, 2017, **523**, 32–38.
- 71 Y. Q. Dang, Y. J. Zhou, J. T. Cai, G. Y. Liu, Y. T. Zhang and J. S. Qiu, *J. Nano Res.*, 2017, **45**, 134–141.
- 72 T. Zhang, H. Xu, W. He, J. Zhu, Z. Yue, B. Xue, B. Dong and H. Song, *RSC Adv*, 2017, **7**, 28987–28993.
- 73 Q. Y. Cai, J. Li, J. Ge, L. Zhang, Y. L. Hu, Z. H. Li and L. B. Qu, *Biosens. Bioelectron.*, 2015, **72**, 31–36.
- 74 X. Yan, Y. Song, C. Zhu, H. Li, D. Du, X. Su and Y. Lin, *Anal. Chem.*, 2018, **90**, 2618–2624.
- 75 C. Yang, W. Deng, H. Liu, S. Ge and Y. Mei, *Sens. Actuators, B*, 2015, **216**, 286–292.
- 76 Y. Hu, L. Zhang, X. Geng, J. Ge, H. Liu and Z. Li, *Anal. Methods*, 2017, **9**, 5653–5658.
- 77 J. Jana, T. Aditya, M. Ganguly and T. Pal, *Sens. Actuators, B*, 2017, **246**, 716–725.
- 78 J. Yang, Z. Huang, Y. Hu, J. Ge, J. Li and Z. Li, *New J. Chem.*, 2018, **42**, 15121–15126.
- 79 D. Garg, A. Mehta, A. Mishra and S. Basu, *Spectrochim. Acta, Part A*, 2018, **192**, 411–419.
- 80 K. Srinivasan, K. Subramanian, K. Murugan and K. Dinakaran, *Analyst*, 2016, **141**, 6344–6352.
- 81 Y. Wang, T. Ma, S. Ma, Y. Liu, Y. Tian, R. Wang, Y. Jiang, D. Hou and J. Wang, *Micro. Acta*, 2017, **184**, 203–210.
- 82 S. Hamd-Ghadareh, A. Salimi, S. Parsa and F. Fathi, *Int. J. Biol. Macromol.*, 2018, **118**, 617–628.
- 83 S. Gogoi and R. Khan, *Phys. Chem. Chem. Phys.*, 2018, **20**, 16501–16509.
- 84 X. Shen, L. Xu, W. Zhu, B. Li, J. Hong and X. Zhou, *New J. Chem.*, 2017, **41**, 9230–9235.
- 85 Z. Li, G. Song, Z. Yuan and L. Chao, *Sens. Actuators, B*, 2017, **241**, 821–827.
- 86 H. Ge, K. Zhang, H. Yu, J. Yue, L. Yu, X. Chen, T. Hou, K. A. Alamry, H. M. Marwani and S. Wang, *J. Fluoresc.*, 2018, **28**, 1405–1412.
- 87 Y.-S. He, C.-G. Pan, H.-X. Cao, M.-Z. Yue, L. Wang and G.-X. Liang, *Sens. Actuators, B*, 2018, **265**, 371–377.
- 88 W. Dong, R. Wang, X. Gong, W. Liang and C. Dong, *Spectrochim. Acta, Part A*, 2019, **213**, 90–96.
- 89 Y. Shi, Y. Pan, H. Zhang, Z. Zhang, M.-J. Li, C. Yi and M. Yang, *Biosens. Bioelectron.*, 2014, **56**, 39–45.
- 90 H. Dai, S. Yan, Y. Wang, Y. Sun, J. Hu, P. Ni and L. Zhuang, *Sens. Actuators, B*, 2014, **202**, 201–208.
- 91 M. Xu, Z. Gao, Z. Qian, Y. Lin, M. Lu and D. Tang, *Biosens. Bioelectron.*, 2016, **86**, 978–984.
- 92 X. Wu, Y. Song, X. Yan, C. Zhu, Y. Ma, D. Du and Y. Lin, *Biosens. Bioelectron.*, 2017, **94**, 292.
- 93 J. Korram, L. Dewangan, R. Nagwanshi, I. Karbhal, K. K. Ghosh and M. L. Satnami, *New J. Chem.*, 2019, **43**, 6874–6882.
- 94 S. Xu, F. Zhang, L. Xu, X. Liu, P. Ma, Y. Sun, X. Wang and D. Song, *Sens. Actuators, B*, 2018, **273**, 1015–1021.
- 95 Y. Yang, D. Huo, H. Wu, X. Wang, J. Yang, M. Bian, Y. Ma and C. Hou, *Sens. Actuators, B*, 2018, **274**, 296–303.
- 96 M. Amjadi, Z. Abolghasemi-Fakhri and T. Hallaj, *J. Photochem. Photobiol., A*, 2015, **309**, 8–14.
- 97 P. A. Sajid, S. S. Chetty, S. Praneetha, A. V. Murugan, Y. Kumar and L. Periyasamy, *RSC Adv*, 2016, **6**, 103482–103490.
- 98 S. Li, J. Wang, W. Sheng, W. Wen, Y. Gu and S. Wang, *Micro. Acta*, 2018, **185**, 388.
- 99 C. Wang, R. Tan and D. Chen, *Talanta*, 2018, **182**, 363–370.
- 100 J.-T. Cao, W.-S. Zhang, H. Wang, S.-H. Ma and Y.-M. Liu, *New J. Chem.*, 2019, **43**, 1424–1430.
- 101 X. Cui, L. Zhu, J. Wu, Y. Hou, P. Wang, Z. Wang and M. Yang, *Biosens. Bioelectron.*, 2015, **63**, 506–512.
- 102 X. Cheng, Y. Cen, G. Xu, F. Wei, M. Shi, X. Xu, M. Sohail and Q. Hu, *Micro. Acta*, 2018, **185**, 144.
- 103 Y. Ding, J. Ling, H. Wang, J. Zou, K. Wang, X. Xiao and M. Yang, *Anal. Methods*, 2015, **7**, 7792–7798.
- 104 X. Fu, L. Sheng, Y. Yu, M. Ma, Z. Cai and X. Huang, *Sens. Actuators, B*, 2018, **269**, 278–287.
- 105 H. Tao, X. Liao, C. Sun, X. Xie, F. Zhong, Z. Yi and Y. Huang, *Spectrochim. Acta, Part A*, 2015, **136**, 1328–1334.
- 106 Y. Wang, H. Meng, M. Jia, Y. Zhang, H. Li and L. Feng, *Nanoscale*, 2016, **8**, 17190–17195.
- 107 M. K. Chini, V. Kumar, A. Javed and S. Satapathi, *Nano-Struct. Nano-Objects*, 2019, **19**, 100347.
- 108 J. Wang, F. Zhang, Y. Wang, Y. Yang and X. Liu, *Carbon*, 2018, **126**, 426–436.